DOI: 10.48011/asba.v2i1.1610

H_2/H_∞ Robust Control Design for Rotary Inverted Pendulum

Luís Felipe Vieira Silva * **Thiago Damasceno Cordeiro** *
Ícaro Bezerra Queiroz de Araújo * **Heitor Judiss Savino** *

* *Institute of Computing, Federal University of Alagoas, AL, (e-mail: felipemmha,thiago,icaro,heitor.savino@ic.ufal.br).*

Abstract: This works presents an H_2/H_∞ robust control scheme for a rotary inverted pendulum using Linear Matrix Inequality (LMI) approach based on Lyapunov theory and taking into account the uncertainty of the position of the pendulum to the servo-basis of the system. The dynamic model of the system is obtained by Euler-Lagrange formulation and the controller is obtained by solving a convex optimization problem. Experiments using this control scheme with changes in the position of the pendulum were made to compare the performance with another controller using pole placement control design. Results show that only H_2/H_∞ controller is able to maintain the stability of the system for all experiments performed in this work.

Keywords: Robust Control Systems, H_2/H_∞ controller, Linear Matrix Inequalities, Rotary Inverted Pendulum, Uncertain Systems.

1. INTRODUCTION

The Rotary Inverted Pendulum (RIP) is a classical problem in the control systems area that provides a challenging platform for control study purposes. Due to the fact that RIP is an unstable multi-variable non-minimum phase system its use is very popular within the control community to verify performance and demonstrating the effectiveness of several control techniques (Cazzolato and Prime, 2011). Moreover, the dynamic model of the RIP is very useful for the study of attitude control of space rockets, automatic aircraft landing systems or for the problem of stabilizing androids (Akhtaruzzaman and Shafie, 2010).

Basically, there are two control tasks for an inverted pendulum system: swing-up and balance control. For swing-up control, the pendulum is swing from its downward stable balance point to the upward unstable balance point. For balance control, the pendulum is in its upright vertical position and the driven arm automatically varies its angle while the controller tries to keep the system stable (Furuta et al., 1992).

The system model is usually determined by energy-based methods, in which differential equations from the mechanical model are obtained by using Euler-Lagrange formulation (Fantoni and Lozano, 2002). However, these mathematical models are just approximations of real physical system and ignore a wide range of uncertainties that can lead to instability such as physical wear on the motor and system gears, problems on the voltage grid, or inaccuracies at the base of the pendulum that have not been properly modeled. For this, robust control theory is used (Zhou et al., 1996).

A robust controller handles two types of problems: the analysis problem and the synthesis problem. For analysis, given a controller, the question is whether the controlled signals satisfy desired properties for all admissible noises, disturbances or model uncertainties. For synthesis, it consists on designing a controller such that the control signals satisfy the desired properties also for noises, disturbances or uncertainties (Zhou and Doyle, 1998).

In the case of RIP, many robust controllers have been studied, most of them based on maintaining stability of the system given modeled disturbances and uncertainties, like H_∞ controller, a method that synthesizes a controller to achieve robust performance or stabilization. Another classical method on robust control design is H_2 controller, which uses H_2 norm as measure for system performance and is useful to deal with measurement noise and random disturbance. A mixed H_2/H_∞ controller consider both: while H_∞ performance is convenient to enforce robustness to model uncertainty, H_2 performance is useful to handle stochastic aspects such as measurement noise and random disturbance.

The purpose of this work is to present a robust H_2/H_∞ controller design that stabilizes the rotary inverted pendulum taking into account uncertainty on the dimensions of the rotary arm.

This work consists of five Sections. Section 2 brings Euler-Lagrange formulation to model the RIP used in this work using state-space representation. Section 3 presents the H_2/H_∞ controller design and discusses about uncertainty in the rotary arm. Experimental results are presented in Section 4 comparing performance of the H_2/H_∞ controller with a pole placement controller. Four experiments are presented using root mean squared error (RMSE) and mean squared error (MSE) as performance indices. Section 5 contains the final conclusions of this work.

2. ROTARY INVERTED PENDULUM MODEL

The RIP used in this work was designed by Quanser Inc. for research and education purposes (Quanser, 2015) with a rotary arm attached to a DC motor (actuator) and the pendulum's rod, which is connected to the rotary arm as can be seen in Figure 1(a).

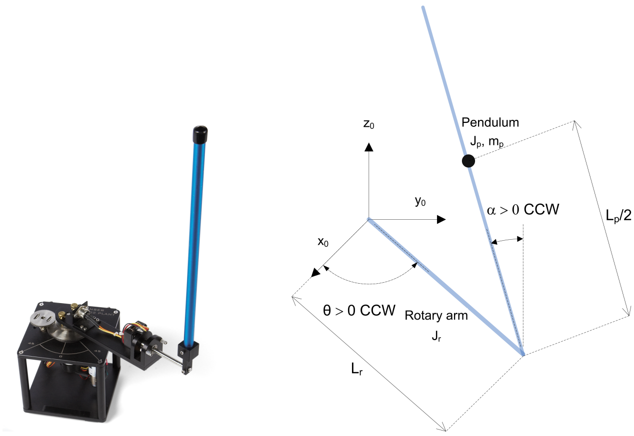

(a) (b)

Figure 1. (a) Rotary inverted pendulum SRV02 ROTPEN designed by Quanser Inc and; (b) Illustrative description of the rotary inverted pendulum.

The rotary arm has length L_r, moment of inertia J_r and its angle to the x_0 axis is θ, which increases positively when the arm is in counter-clockwise (CCW) rotation. The pendulum's rod has length L_p and its center of mass is located in $L_p/2$ with moment of inertia J_p. The angle of the pendulum's rod, α, is zero when it is perfectly aligned on the vertical (z_0 axis) and increases positively when it is rotated counter-clockwise, as can be seen in Figure 1(b).

Two equations of motion are provided in the case of Quanser's RIP (Quanser, 2011), which are obtained using Lagrange method. The entire formulation can be found in (Vieira, 2019) and these two equations are derived as

$$\begin{aligned}&\left(m_pL_r^2+\frac{1}{4}m_pL_p^2-\frac{1}{4}m_pL_p^2\,(\cos\alpha)^2+J_r\right)\ddot{\theta}\\&-\left(\frac{1}{2}m_pL_pL_r\cos\alpha\right)\ddot{\alpha}+\left(\frac{1}{2}m_pL_p^2\sin\alpha\cos\alpha\right)\dot{\theta}\dot{\alpha}\\&+\left(\frac{1}{2}m_pL_pL_r\sin\alpha\right)\dot{\alpha}^2=\tau-B_r\dot{\theta},\end{aligned}\tag{1}$$

$$\begin{aligned}&-\frac{1}{2}m_pL_pL_r\cos\alpha\ddot{\theta}+\left(J_p+\frac{1}{4}m_pL_p^2\right)\ddot{\alpha}\\&-\frac{1}{4}m_pL_p^2\cos\alpha\sin\alpha\dot{\theta}^2-\frac{1}{2}m_pL_pg\sin\alpha=-B_p\dot{\alpha}.\end{aligned}\tag{2}$$

A linear state-space model of this system can be reached using Taylor series (Quanser, 2011). The resulting linear equations, with initial conditions $\theta_0=\alpha_0=\dot{\theta}_0=\dot{\alpha}_0=0$ are as follows:

$$(m_pL_r^2+J_r)\ddot{\theta}-\frac{1}{2}m_pL_pL_r\ddot{\alpha}=\tau-B_r\dot{\theta}.\tag{3}$$

$$\begin{aligned}&\frac{1}{2}m_pL_pL_r\ddot{\theta}+\left(J_p+\frac{1}{4}m_pL_p^2\right)\ddot{\alpha}\\&-\frac{1}{2}m_pL_pg\alpha=-B_p\dot{\alpha}.\end{aligned}\tag{4}$$

The resulting matrix is

$$\begin{aligned}&\begin{bmatrix}m_pL_r^2+J_r & -\frac{1}{2}m_pL_pL_r\\ -\frac{1}{2}m_pL_pL_r & J_p+\frac{1}{4}m_pL_p^2\end{bmatrix}\begin{bmatrix}\ddot{\theta}\\ \ddot{\alpha}\end{bmatrix}+\begin{bmatrix}B_r & 0\\ 0 & B_p\end{bmatrix}\begin{bmatrix}\dot{\theta}\\ \dot{\alpha}\end{bmatrix}\\&+\begin{bmatrix}0\\ -\frac{1}{2}m_pL_pg\alpha\end{bmatrix}=\begin{bmatrix}\tau\\ 0\end{bmatrix}.\end{aligned}\tag{5}$$

Reorganizing Equation (5), the following matrix is obtained:

$$\begin{bmatrix}m_pL_r^2+J_r & \frac{1}{2}m_pL_pL_r\\ -\frac{1}{2}m_pL_pL_r & Jp+\frac{1}{4}m_pL_p^2\end{bmatrix}\begin{bmatrix}\ddot{\theta}\\ \ddot{\alpha}\end{bmatrix}=\begin{bmatrix}\tau-B_r\dot{\theta}\\ \frac{1}{2}m_pL_pg\alpha-B_p\dot{\alpha}\end{bmatrix}.\tag{6}$$

Thus, $\ddot{\theta}$ and $\ddot{\alpha}$ can be expressed as

$$\begin{aligned}\ddot{\theta}=&\frac{1}{J_T}(-(J_p+\frac{1}{4}m_pL_p^2)B_r\dot{\theta}-\frac{1}{2}m_pL_pL_rB_p\dot{\alpha}\\&+\frac{1}{4}m_p^2L_p^2L_rg\alpha+(J_p+\frac{1}{4}m_pL_p^2)\tau)\end{aligned}\tag{7}$$

and

$$\begin{aligned}\ddot{\alpha}=&\frac{1}{J_T}(-\frac{1}{2}m_pL_pL_rB_r\dot{\theta}-(J_r+m_pL_r^2)B_p\dot{\alpha}\\&+\frac{1}{2}m_pL_pg(J_r+m_pL_r^2)\alpha+\frac{1}{2}m_pL_pL_r\tau).\end{aligned}\tag{8}$$

with $1/J_T=J_pm_pL_r^2+J_rJ_p+\frac{1}{4}J_rm_pL_p^2$. To put the system in a state-space form, the state vector x for the rotary pendulum system is defined such as

$$x^T=[x_1\ x_2\ x_3\ x_4]=[\theta\ \alpha\ \dot{\theta}\ \dot{\alpha}]\tag{9}$$

The state vector (9) shows that $\dot{x_1}=x_3$ and $\dot{x_2}=x_4$. Replacing this into (7) and (8), and making $u=\tau$, it gives

$$\begin{aligned}\dot{x_3}=&\frac{1}{J_T}(-(J_p+\frac{1}{4}m_pL_p^2)B_rx_3-\frac{1}{2}m_pL_pL_rB_px_4\\&+\frac{1}{4}m_p^2L_p^2L_rgx_2+(J_p+\frac{1}{4}m_pL_p^2)u)\end{aligned}\tag{10}$$

and

$$\begin{aligned}\dot{x_4}=&\frac{1}{J_T}(-\frac{1}{2}m_pL_pL_rB_rx_3-(J_r+m_pL_r^2)B_px_4\\&+\frac{1}{2}m_pL_pg(J_r+m_pL_r^2)x_2+\frac{1}{2}m_pL_pL_ru).\end{aligned}\tag{11}$$

Thus, matrices A and B in $\dot{x}=Ax+Bu$ formulation are

$$A=\frac{1}{J_T}\begin{bmatrix}0 & 0 & J_T & 0\\ 0 & 0 & 0 & J_T\\ 0 & a_{32} & a_{33} & a_{34}\\ 0 & a_{42} & a_{43} & a_{44}\end{bmatrix},\tag{12}$$

where

$$a_{32} = \frac{1}{4} m_p^2 L_p^2 L_r g,$$
$$a_{33} = -(J_p + \frac{1}{4} m_p L_p^2) B_r,$$
$$a_{34} = \frac{1}{2} m_p L_p L_r B_p,$$
$$a_{42} = \frac{1}{2} m_p L_p g (J_r + m_p L_r^2),$$
$$a_{43} = -\frac{1}{2} m_p L_p L_r B_r,$$
$$a_{44} = -(J_r + m_p L_r^2) B_p,$$

and

$$B = \frac{1}{J_T} \begin{bmatrix} 0 \\ 0 \\ J_p + \frac{1}{4} m_p L_p^2 \\ \frac{1}{2} m_p L_p L_r \end{bmatrix}. \quad (13)$$

.

All the given parameters of the RIP can be found in (Inc., 2012; Quanser, 2015). Using these values, and for $L_r = 0.2159$, the state matrix A is given by

$$A = \begin{bmatrix} 0 & 0 & 1 & 0 \\ 0 & 0 & 0 & 1 \\ 0 & 80.3 & -45.8 & -0.930 \\ 0 & 122 & -44.1 & -1.40 \end{bmatrix}, \quad (14)$$

input matrix B is given by

$$B = \begin{bmatrix} 0 \\ 0 \\ 83.4 \\ 80.3 \end{bmatrix}. \quad (15)$$

Only the servo position and link angles are measured in the output equation. Therefore, matrices C and D are given by

$$C = \begin{bmatrix} 1 & 0 & 0 & 0 \\ 0 & 1 & 0 & 0 \end{bmatrix} \text{ and } D = \begin{bmatrix} 0 \\ 0 \end{bmatrix}, \quad (16)$$

and the output equation $y = Cx + Du$ is given by

$$y = \begin{bmatrix} 1 & 0 & 0 & 0 \\ 0 & 1 & 0 & 0 \end{bmatrix} x = \begin{bmatrix} x_1 \\ x_2 \end{bmatrix} \quad (17)$$

The system's open-loop poles are thus $s_1 = 0$, $s_2 = -48.41$, $s_3 = 7.05$, and $s_4 = -5.86$.

2.1 The rotary arm uncertain model

The rotary arm length is measured from the pendulum's rod to the base of the servo and equals to $L_r = 0.216$m. However, this parameter can be in a range of $0.16 - 0.216$m leading to the following research question: is it possible to stabilize the closed-loop system, using a controller with static gains, taking into account the range of the rotary arm length (L_r) uncertainties? The RIP model with uncertainties can be represented by the following equation:

$$\begin{aligned} \dot{x}(t) &= A(L_r)x(t) + B_u(L_r)u(t) + B_w w(t), \\ z(t) &= Cx(t), \end{aligned} \quad (18)$$

where L_r is limited to $\mathcal{R} = \{L_r \in \mathbb{R} \mid 0.16 \le L_r \le 0.216\}$.

As an example, for $L_r = 0.16$ m, matrices A and B have the new following values:

$$A(L_r = 0.16) = \begin{bmatrix} 0 & 0 & 1 & 0 \\ 0 & 0 & 0 & 1 \\ 0 & 60.3 & -45.8 & -0.69 \\ 0 & 74.9 & -32.6 & -0.85 \end{bmatrix}, \quad (19)$$

and

$$B(L_r = 0.16) = \begin{bmatrix} 0 \\ 0 \\ 83.4 \\ 59.5 \end{bmatrix}. \quad (20)$$

The new system's open-loop poles are $s_1 = 0$, $s_2 = -47.26$, $s_3 = 5.86$ and $s_4 = -5.28$.

3. H_2/H_∞ ROBUST CONTROL DESIGN FOR ROTARY INVERTED PENDULUM

The H_2 and H_∞ controllers can be combined in a central H_2/H_∞ controller that minimizes H_2 norm from disturbance signal $w(t)$ to controlled output $z(t)$, while also guaranteeing disturbance attenuation H_∞.

Consider the following linear system:

$$\begin{aligned} \dot{x}(t) &= Ax(t) + B_u u(t) + B_w w(t) \\ z(t) &= C_z x(t) + D_{zu} u(t) + D_{zw} w(t), \end{aligned} \quad (21)$$

where $x(t) \in \mathbb{R}^n$ is the state vector, $z(t) \in \mathbb{R}^p$ is the output vector, $w(t) \in \mathbb{R}^q$ is the disturbance vector and $u(t) \in \mathbb{R}^m$ is the input control vector. A, B_u, B_w, C_z, D_{zu} and D_{zw} are the system coefficient matrices of appropriate dimensions. For a state-feedback matrix $K \in \mathbb{R}^{p \times n}$ such that $u(t) = -Kx(t)$, and considering $D_{zu} = D_{zw} \equiv 0$, (21) can be rewritten as the new system

$$\begin{aligned} \dot{x}(t) &= A'x(t) + B_w w(t) \\ z(t) &= C'_z x(t), \end{aligned} \quad (22)$$

where $A' = (A - B_u K)$ and $C'_z = (C_z - D_{zu} K)$, $C_z = C$ and $B_w = 0$.

3.1 H_2 Controller

The H_2 problem is how to determine a gain matrix K, that stabilizes system (22) with minimum H_2 norm. It must be remembered that the H_2 norm of the system (22) is determined by the following optimization problem:

$$min\ Tr\Big[C'_z Q (C'_z)^T\Big] : \begin{cases} Q = Q^T > 0 \\ (A')Q + Q(A')^T + B_w B_w^T < 0 \end{cases} \quad (23)$$

However, as the objective function and the LMI of (23) has non convex terms, the following relations will be used (Duan and Yu, 2013):

- $W \ge C'_z Q (C'_z)^T$;
- $Y = KQ$.

With these relations, and using Schur's complement in (23), a theorem for H_2 control using state feedback can be written.

Theorem 1. (H_2 control). Consider system (22). If there exist a symmetric matrix Q and two symmetric matrices W and Y such that:

$$\min\ Tr(W): \begin{cases} \begin{bmatrix} W & (C_zQ - D_{zu}Y) \\ (QC_z^T - Y^T D_{zu}^T) & Q \end{bmatrix} \geq 0, \\ \\ \begin{bmatrix} b_{11} & B_w \\ B_w^T & -I \end{bmatrix} < 0, \end{cases} \tag{24}$$

where $b_{11} = (AQ + QA^T - B_uY - Y^T B_u^T)$ and I is a identity matrix of order 1. Then the system is stable for the control law $u(t) = -YQ^{-1}x(t)$ and the H_2 norm of the system is $\| G_{wz} \|_2 < \sqrt{Tr(W)}$.

3.2 H_∞ Controller

The H_∞ problem is how to determine a gain matrix K, that stabilizes system (22) with minimum H_∞ norm. Thus, a theorem of H_∞ control using state feedback can be written (Palhares and Gonçalves, 2007).

Theorem 2. (H_∞ control). Consider system (22). If there exist a symmetric matrix Q and a scalar $\delta > 0$ such that:

$$\min\ \delta: \begin{cases} Q = Q^T > 0, \\ \\ \begin{bmatrix} a_{11} & B_w & (QC_z^T - Y^T D_{zu}^T) \\ B_w^T & -\delta I & D_{zw}^T \\ (C_zQ - D_{zu}Y) & D_{zw} & -I \end{bmatrix} < 0, \end{cases} \tag{25}$$

where $a_{11} = AQ + QA^T - B_uY - Y^T B_u^T$ and $\delta \equiv \gamma^2$. Then, system (22) is stabilized by the control law $u(t) = -YQ^{-1}x(t)$ and the H_∞ norm of this system is given by $\| G_{wz} \|_\infty = \sqrt{\delta} = \gamma$.

3.3 H_2/H_∞ Controller

As mentioned before, an H_2/H_∞ controller is a combination of both H_2 and H_∞ controllers. Therefore, a theorem of this control strategy can be defined as follows.

Theorem 3. (H_2/H_∞ control). Consider system (22). If there exist a symmetric matrix Q and a scalar $\delta > 0$ such that:

$$\min\ Tr(W): \begin{cases} Q = Q^T > 0, \\ \\ \begin{bmatrix} W & a_{12} \\ a_{21} & Q \end{bmatrix} \geq 0, \\ \\ \begin{bmatrix} b_{11} & B_w & b_{13} \\ B_w^T & -\delta I & D_{zw}^T \\ b_{31} & D_{zw} & -I \end{bmatrix} < 0, \end{cases} \tag{26}$$

where $a_{12} = (C_zQ - D_{zu}Y)$, $a_{21} = a_{12}^T$, $b_{13} = QC_z^T - Y^T D_{zu}^T$, $b_{31} = b_{13}^T$ and $b_{11} = AQ + QA^T - B_uY - Y^T B_u^T$. Then, the system is stabilized by the control law

$$u(t) = -YQ^{-1}x(t), \tag{27}$$

where the H_∞ norm of the system is $\| G_{wz} \|_\infty < \sqrt{\delta} < \gamma$ and the H_2 norm is $\| G_{wz} \|_2 < \sqrt{Tr(W)}$.

3.4 Control Signal Restrictions

In some cases, the optimum gain of an H_∞ controller can assume a very high norm value. This case may not be acceptable for real systems and the use of saturation in the control signal is required, e.g., in DC motor input voltage (V_m). The usual solution for this problem is to impose limitations on the control signal $u(t) = -Kx(t)$. For this, consider the following conditions:

- There are two matrices $Q > 0$ and Y that satisfy Theorem 2 [1].
- The *i-th* control signal $u_i(t)$, $i = \{1, ..., p\}$, should be limited between $\pm\mu$.

From the conditions above and knowing that $u(t) = -YQ^{-1}x(t)$, then

$$\begin{array}{rcl} \max\limits_{t\leq 0} \| u_i \| & \leq & \mu_i \iff \\ \max\limits_{t\leq 0} \| K_i x(t) \| & \leq & \max\limits_{t\leq 0} \| Y_i Q^{-1} x \| \\ & \leq & \| Y_i Q^{-\frac{1}{2}} \| \max\limits_{t\leq 0} \| Q^{-\frac{1}{2}} x \| \\ & \leq & \sqrt{\lambda_{\max}(Q^{-\frac{1}{2}} Y_i^T Y_i Q^{-\frac{1}{2}})} \ \leq \mu_i \end{array}, \tag{28}$$

where $K_i(Y_i)$ is the *i-th* line of matrix $K(Y)$ and $\lambda_{\max}(*)$ is the maximum eigenvalue of $(*)$ (Trofino, 2000). Therefore, the restriction $\| u_i \|$, is equivalent to the following LMI, $\forall i$:

$$\begin{bmatrix} Q & Y_i^T \\ Y_i & \mu_i^2 \end{bmatrix} \geq 0. \tag{29}$$

This LMI constraint can be used in conjunction with H_2, H_∞ and H_2/H_∞ control constraints so that the solution of the convex optimization problem can find the same matrices Q and Y that satisfy all imposed conditions.

Otherwise, if the optimum gain from the controller and its H_∞ norm are very small, the gain may not be enough to turn on a real system. This problem can be solved in a simple way by imposing another LMI with a positive constraint on the matrix that makes up the K gain, i.e., for $K = YQ^{-1}$ it is possible to impose the following relationship:

$$Q = Q^T > \epsilon I, \tag{30}$$

where $\epsilon > 0$ is a very small scalar. This solution generates a sub-optimal controller that must be evaluated at control design (Palhares et al., 1998).

For each n uncertainties in a model, it is generated a polytope $\mathcal{B}_n$ with 2^n vertices. Given the number of uncertainties and its range of values, an algorithm can be implemented [2] to generate all A, B, C, and D matrices on the vertices of a polytope. Since only the uncertainty of L_r was modeled, a polytope $\mathcal{B}_1$ was generated with two vertices.

In H_2/H_∞ robust control, the conditions from Theorem 3 must be satisfied for each system configuration on the vertices of $\mathcal{B}_1$. To avoid very high voltages, a constraint of $\pm 5V$ is added to the control variable, since these values are sufficient to control the system. For very small norm values, making the controlled system very slow, a positivity constraint can be added in the matrix to increase the K gain. Empirically, a reasonable ϵ value obtained was 0.375. Thus, the final convex optimization problem to obtain the H_2/H_∞ controller with limitation on the control variable and sub-optimal norm is to minimize $Tr(W)$ subject to

[1] Also valid to H_2 and H_2/H_∞ Theorems (1 and 3, respectively)

[2] The implementation can be found at https://github.com/lfelipev/robust-control

$$Q = Q^T > \epsilon I,$$

$$\begin{bmatrix} W & a_{12} \\ a_{21} & Q \end{bmatrix} \geq 0,$$

$$\begin{bmatrix} b_{11} & B_w(n) & b_{13} \\ B_w^T & -\delta I & D_{zw}(n)^T \\ b_{31} & D_{zw}(n) & -I \end{bmatrix} < 0, \quad . \tag{31}$$

$$\begin{bmatrix} Q & Y^T \\ Y & \mu^2 \end{bmatrix} \geq 0,$$

where n is the n-th system on the polytope vertice, $a_{12} = C_z(n)Q - D_{zu}(n)Y$, $a_{21} = a_{12}^T$, $b_{11} = A(n)Q + QA(n)^T - B_u(n)Y - Y^T B_u(n)^T$, $b_{13} = QC_z(n)^T - Y^T D_{zu}(n)^T$, and $b_{31} = b_{13}^T$.

4. RESULTS

Problem (31) has been solved using **SeDuMi** (Sturm, 1999), a computational optimization package restricted to symmetric matrix cones that can be used to find matrix Q to minimize $Tr(W)$.

The H_∞ norm is $\sqrt{\delta} = \gamma = 5.09$, the H_2 norm is $\sqrt{Tr(W)} = 1.55$, and the RIP is controlled by the control law $u(t) = -YQ^{-1}x(t) = -K_{H_2/H_\infty}x(t)$.

The designed control gains are

$$K_{H_2/H_\infty} = [-5.57 \ 26.92 \ -2.98 \ 4.21], \tag{32}$$

and the closed-loop poles are calculated as $-3.49 \pm j5.10$, -4.26, and -1251. These results were computed with MATLAB R2014b running in Windows 10, Intel Core-i5 CPU at 3.1GHz, and 8GB RAM.

The values of Q and Y were calculated as follows:

$$Q = \begin{bmatrix} 0.0026 & -0.0005 & -0.0092 & 0.0011 \\ -0.0005 & 0.0037 & 0.0092 & -0.0178 \\ -0.0092 & 0.0092 & 0.1565 & 0.0356 \\ 0.0011 & -0.0178 & 0.0356 & 0.1389 \end{bmatrix} * 10^{-6}, \tag{33}$$

$$Y = [0.0310 \ 0.0074 \ -0.1769 \ -0.0653] * 10^{-7}. \tag{34}$$

To evaluate the performance of the H_2/H_∞ robust controller on the SRV02 RIP, a state-feedback controller designed through pole-placement is used (Quanser, 2015). The gain vector of this controller is $K_Q = [-5.26 \ 28.16 \ -2.76 \ 3.22]$ with closed-loop poles $-2.80 \pm j2.86$, -30, -40. This controller was designed to obtain the following system specifications:

- Damping ratio: $\zeta = 0.7$;
- Natural frequency: $\omega_n = 4rad/s$;

In all performed experiments, the pendulum starts in a hanging down position and the RIP angle is ±180. Then, it is manually brought to the upright position, with the angle going up to zero, and the controller starts to work.

Four experiments were done to evaluate the performance of the two controllers. The first consists of positioning the rotary arm at $L_r = 0.17$ m from the base of the servo and varying the angle θ by $\pm10°$. The second consists of positioning the rotary arm at $L_r = 0.21$ m from the base of the servo with the same variation of the angle θ. The third experiment was done with the rotary arm at $L_r = 0.21$ m and varying the angle θ by $\pm20°$ and the fourth experiment was done by placing the rotary arm at $L_r = 0.17$ m with the angle θ varying at $\pm20°$.

Two performance indices were used: *mean squared error* (MSE) and *root mean squared error* (RMSE) (Chai and Draxler, 2014). The quadratic scoring rules that measures average magnitude of the error are given by

$$RMSE = \sqrt{MSE} = \sqrt{\frac{1}{n}\sum_{i=1}^{n} e_i^2}. \tag{35}$$

.

4.1 Experiment 1: Rotary arm $L_r = 0.17$ m and $\theta = \pm10°$

Positioning the rotary arm in 0.17 m from the base of the servo and varying θ between $\pm10°$, the simulation results are showed in Figure 2 with 20 seconds of simulation. The same result is shown with the time between 9.5 and 13 seconds in Figure 3 for better visualization.

From these figures, it can be seen that the controller with the K_Q gains (dotted lines) have shown an oscillatory behavior before being able to put the angle α at zero degrees. This oscillatory behavior was seen in the control variable V_m, represented in gray color, in the pendulum's rod angle (α) and in the angle of the rotary arm (θ). As can be seen, controller H_2/H_∞ (the continuous lines) manages to stabilize near the equilibrium point more quickly, although it still has a low θ oscillation.

The performance indices MSE and RMSE can be seen in the Table 1. The angle α and control input V_m were calculated in relation to the balance point (zero). MSE and RMSE of θ were calculated in relation to the reference ($\pm10°$) represented in Figures 2 and 3 by the dashed line. Ignoring the initial conditions of the system, the calculations were made after 2 seconds of simulation, which is the time before the pendulum being lifted.

Table 1. Performance indices comparison for pole-placement controller (K_Q) and H_2/H_∞ controller (K_{H_2/H_∞}) for $L_r = 0.17m$ and $\theta = \pm10°$.

Performance Index	K_Q	K_{H_2/H_∞}
MSE α	5.10	1.75
RMSE α	2.25	1.32
MSE θ	42.07	33.55
RMSE θ	6.48	5.79
MSE V_m	0.76	0.24
RMSE V_m	0.87	0.49

4.2 Experiment 2: Rotary arm $L_r = 0.21$ m and $\theta = \pm10°$

Positioning the rotary arm at 0.21 m from the base of the servo and varying the angle θ between $\pm10°$, the simulation results are shown in Figure 4 with a simulation time of 20 seconds and also with time between 9.5 and 13 seconds in Figure 5.

It can be seen that the angle transition is more smooth. However, the H_2/H_∞ controller presented a greater overshoot in the angle θ that influenced the performance indices calculation. The performance of the controllers can

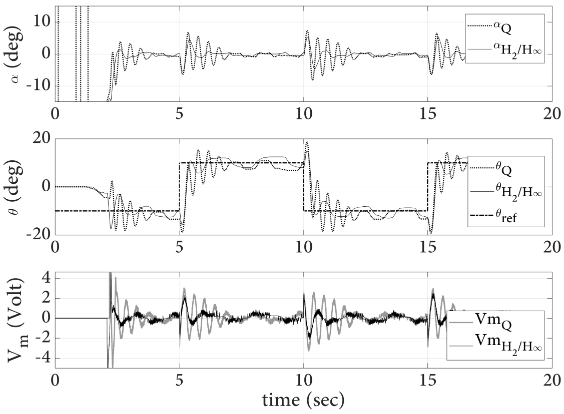

Figure 2. Experimental result with the rotary arm angle (θ) varying between $\pm 10°$ and the distance between the servo and the pendulum equal to 0.17 m. Simulation result with time between 0 and 20 seconds.

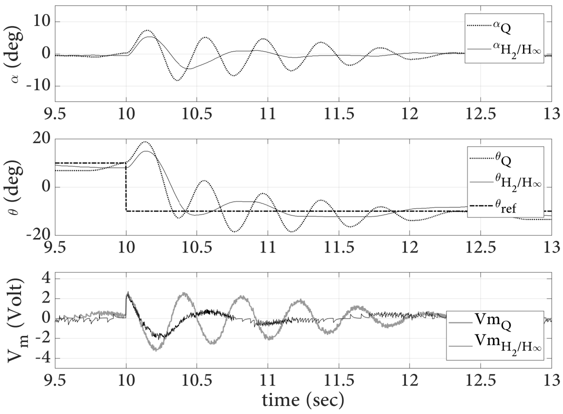

Figure 3. Experimental result with the rotary arm angle (θ) varying between $\pm 10°$ and the distance between the servo and the pendulum equal to 0.17 m. Simulation result with time between 9.5 and 13 seconds.

be seen in Table 2. Both MSE and RMSE of α, V_m and θ are calculated as in experiment 1, i.e., ignoring the first 2 seconds of simulation due to initial conditions. The angle α and the control signal V_m showed similar values, but in the angle θ the MSE and RMSE were higher for H_2/H_∞ controller. It can be concluded that the values were almost the inverse of experiment 1 for the angle θ.

Table 2. Performance indices comparison for pole-placement controller (K_Q) and H_2/H_∞ controller (K_{H_2/H_∞}) for $L_r = 0.21m$ and $\theta = \pm 10°$.

Performance Index	K_Q	K_{H_2/H_∞}
MSE α	1.04	1.48
RMSE α	1.02	1.22
MSE θ	33.65	40.90
RMSE θ	5.80	6.39
MSE V_m	0.16	0.17
RMSE V_m	0.40	0.42

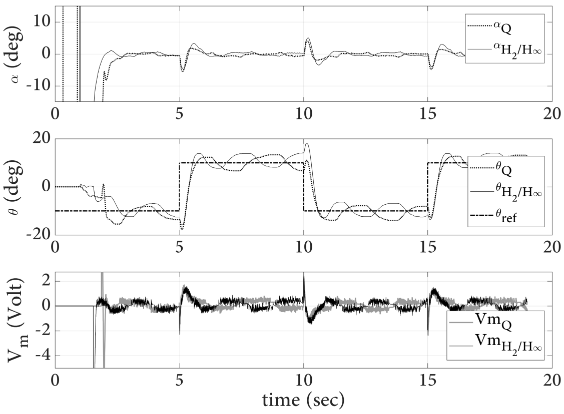

Figure 4. Experimental result with the rotary arm angle (θ) varying between $\pm 10°$ and the distance between the servo and the pendulum equal to 0.21 m. Simulation result with time between 0 and 20 seconds.

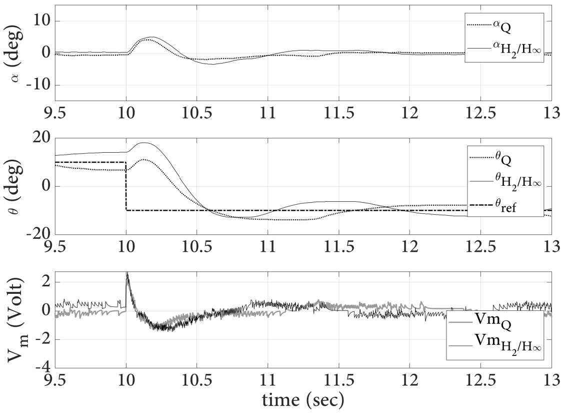

Figure 5. Experimental result with the rotary arm angle (θ) varying between $\pm 10°$ and the distance between the servo and the pendulum equal to 0.21 m. Simulation result with time between 9.5 and 13 seconds.

4.3 Experiment 3: Rotary arm $L_r = 0.21$ m and $\theta = \pm 20°$

In this experiment the rotary arm was positioned at $L_r = 0.21$ m from the servo base and the variation of the angle θ was $\pm 20°$. This means that the DC motor input voltage, V_m, will have higher peaks to execute the change of angle. The simulation results with 20 seconds of simulation are displayed in Figure 6. The same result is shown in Figure 7 between 9.5 and 13 seconds.

In this experiment, both controllers showed a very similar behavior for both angles θ and α and also for control input V_m including higher voltage peaks needed to make the angle transitions.

The performance indices of the controllers can be seen in Table 3, the MSE and RMSE of α, V_m, and θ were also calculated despising the first 2 seconds of simulation due to initial conditions.

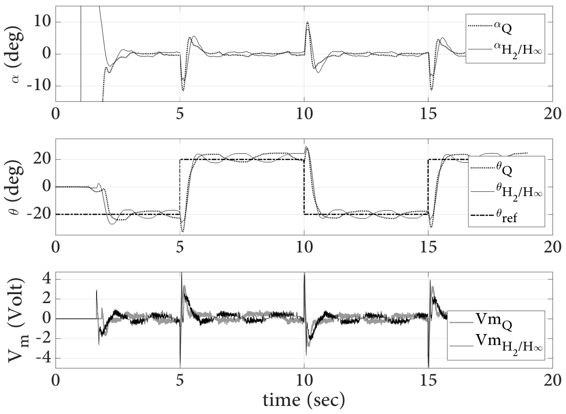

Figure 6. Experimental result with the rotary arm angle (θ) varying between $\pm 20°$ and the distance between the servo and the pendulum equal to 0.21 m. Simulation result with time between 0 and 20 seconds.

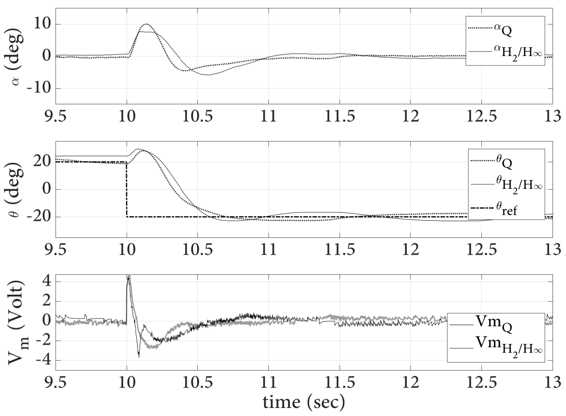

Figure 7. Experimental result with the rotary arm angle (θ) varying between $\pm 20°$ and the distance between the servo and the pendulum equal to 0.21 m. Simulation result with time between 9.5 and 13 seconds.

Table 3. Performance indices comparison for pole-placement controller (K_Q) and H_2/H_∞ controller (K_{H_2/H_∞}) for $L_r = 0.21m$ and $\theta = \pm 20°$.

Performance Index	K_Q	K_{H_2/H_∞}
MSE α	3.93	3.89
RMSE α	1.98	1.97
MSE θ	114.17	116.53
RMSE θ	10.68	10.79
MSE V_m	0.45	0.42
RMSE V_m	0.67	0.65

4.4 Experiment 4: Rotary arm $L_r = 0.17$ m and $\theta = \pm 20°$

In this experiment the rotary arm was positioned at $L_r = 0.21$ m from the servo base and the variation in the angle θ was $\pm 20°$. Because of high variation in angle θ it is also expected that the controller voltage will have higher peaks to execute the change of angle. The simulation results are showed in Figure 8 with 20 seconds and in Figure 9 with time between 9.5 and 13 seconds.

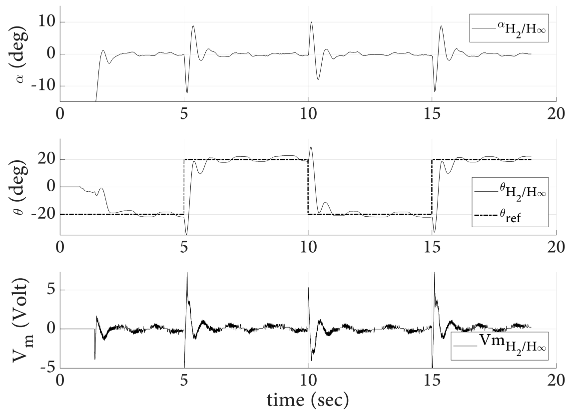

Figure 8. Experimental result with the rotary arm angle (θ) varying between $\pm 20°$ and the distance between the servo and the pendulum equal to 0.17 m. Simulation result with time between 0 and 20 seconds.

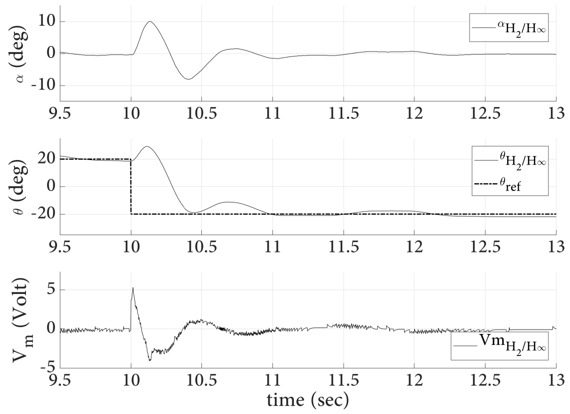

Figure 9. Experimental result with the rotary arm angle (θ) varying between $\pm 20°$ and the distance between the servo and the pendulum equal to 0.17 m. Simulation result with time between 9.5 and 13 seconds.

In this experiment only the H_2/H_∞ controller remained stable. The controller by pole-placement wasn't able to control the system in this configuration. Although the controller output voltage was limited in $\pm 5V$, the figures show that the system needed voltage peaks above $5V$ in a short period of time when changing the angle.

The performance indices of the H_2/H_∞ controller can be seen in Table 4. The MSE and RMSE of α, V_m, and θ are calculated similarly to experiment 1, despising the first 2 seconds of simulation due to initial conditions.

5. CONCLUSION

This work presented the modeling and control of a rotary inverted pendulum. The Euler-Lagrange formulation was used to obtain the mathematical model of the pendulum. With this model and its representation in state-space, two control techniques were applied: pole-placement and H_2/H_∞ robust control.

Table 4. Performance indices comparison for pole-placement controller (K_Q) and H_2/H_∞ controller (K_{H_2/H_∞}) for $L_r = 0.17m$ and $\theta = \pm 20°$.

Performance Index	K_{H_2/H_∞}
MSE α	4.69
RMSE α	2.16
MSE θ	103.09
RMSE θ	10.15
MSE V_m	0.73
RMSE V_m	0.85

The main objective of this work is to implement and evaluate the performance of the H_2/H_∞ controller in a rotary inverted pendulum system. The study was made taking into account the uncertainty of the position of the rotary arm in a range of $0.17 - 0.21$ m.

Experimental results showed the practical application of robust control theory, where an H_2/H_∞ controller managed to maintain pendulum stability even in the presence of modeled uncertainty in four different scenarios. The pole-placement controller only showed robustness for three of the four experiments performed while the H_2/H_∞ controller has fulfilled its objective. As future works, it will be considered to implement robust controllers that guarantee not only stability, but other performance indices in the controller design projects like steady-state error, rising-time, overshoot etc.

REFERENCES

Akhtaruzzaman, M. and Shafie, A.A. (2010). Modeling and control of a rotary inverted pendulum using various methods, comparative assessment and result analysis. In *2010 IEEE International Conference on Mechatronics and Automation*, 1342–1347.

Cazzolato, B.S. and Prime, Z. (2011). On the dynamics of the furuta pendulum. *Journal of Control Science and Engineering*, 2011.

Chai, T. and Draxler, R.R. (2014). Root mean square error (rmse) or mean absolute error (mae)?–arguments against avoiding rmse in the literature. *Geoscientific model development*, 7(3), 1247–1250.

Duan, G.R. and Yu, H.H. (2013). *LMIs in control systems: analysis, design and applications*. CRC press.

Fantoni, I. and Lozano, R. (2002). Stabilization of the furuta pendulum around its homoclinic orbit. *International Journal of Control*, 75(6), 390–398.

Furuta, K., Yamakita, M., and Kobayashi, S. (1992). Swing-up control of inverted pendulum using pseudo-state feedback. *Proceedings of the Institution of Mechanical Engineers, Part I: Journal of Systems and Control Engineering*, 206(4), 263–269.

Inc., Q. (2012). *Inverted Pendulum Experiment User Manual*.

Palhares, R., De Oliveira, S., Peres, P., et al. (1998). Relating two state feedback h∞ control approaches. *Controle and Automacao*.

Palhares, R. and Gonçalves, E. (2007). Desigualdades matriciais lineares em controle. *Enciclopédia de Automática: Controle & Automação*, 1, 155–195.

Quanser (2011). *Rotary Pendulum Workbook*.

Quanser (2015). *SRV02 Rotary Servo Base Unit User Manual*.

Sturm, J.F. (1999). Using SeDuMi 1.02, a matlab toolbox for optimization over symmetric cones. *Optimization Methods and Software*, 11(1-4), 625–653.

Trofino, A. (2000). Controle robusto. 2000. *Apostila–Programa de Pós-Graduação em Engenharia Elétrica Laboratório de Controle e Micro-Informática, Universidade Federal de Santa Catarina, Florianópolis.*

Vieira, L.F.S. (2019). H_2/H_∞ Robust Control Design for Rotary Inverted Pendulum. Monografia (Bacharel em Engenharia de Computação), UFAL (Universidade Federal de Alagoas), Alagoas, Brasil.

Zhou, K. and Doyle, J.C. (1998). *Essentials of robust control*, volume 104. Prentice hall Upper Saddle River, NJ.

Zhou, K., Doyle, J.C., Glover, K., et al. (1996). *Robust and optimal control*, volume 40. Prentice hall New Jersey.